Kink's internal modes in the Frenkel-Kontorova model

Oleg M. Braun
Institute of Physics, The Ukrainian Academy of Sciences, 46 Science Avenue, Kiev 252022, Ukraine

Yuri S. Kivshar
Optical Sciences Center, Research School of Physical Sciences and Engineering, The Australian National University, Canberra, Australian Capital Territory 0200, Australia

Michel Peyrard
Laboratoire de Physique de l'Ecole Normale Supérieure de Lyon, 46 Allée d'Italie, 69364 Lyon Cédex 07, France
(Received 29 April 1997)

We consider a generalized Frenkel-Kontorova model, describing the dynamics of a chain of particles in a periodic substrate potential, and analyze the effect of discreteness on the existence and properties of internal (or shape) modes of kinks, topological excitations of the chain. In particular, we show that kink's internal modes can appear *not only below* but *also above* the phonon spectrum band and, in the latter case, the localized mode describes out-of-phase oscillations of the kink's shape. For the sinusoidal on-site potential, when the model is described by the discrete sine-Gordon equation, we reveal, in sharp contrast with the continuum limit, the existence of the kink's internal mode in a narrow region of the discreteness parameter. We apply two different analytical techniques to describe the cases of weak and strong coupling between particles, explaining qualitatively and even quantitatively the main features of the kink oscillations observed in numerical simulations. We also discuss the effect of nonlinearity on the existence and properties of kink's internal modes and show, in particular, that a nonlinearity-induced frequency shift of the lattice vibrations can lead to the creation of the *nonlinear kink's internal modes*, which, however, slowly decay due to a generation of radiation through higher-order harmonics. [S1063-651X(97)11010-8]

PACS number(s): 46.10.+z, 63.20.Ry, 66.30.Hs, 03.40.Kf

I. INTRODUCTION

The well-known Frenkel-Kontorova (FK) model, first introduced in 1938 for describing dislocations in solids [1], was successfully used in investigations of a number of physical phenomena such as charge-density waves, adsorbed layers of atoms, domain walls in ferro- and antiferromagnetic systems, crowdions in metals, and hydrogen-bonded molecules (see, e.g., the review paper [2] and reference therein). The classical FK model describes a chain of linearly coupled particles (''atoms'') subjected to an external periodic substrate potential $V_{\rm sub}(u)$. The Hamiltonian of the FK model can be written in the form

$$H=\sum_l \left[\frac{1}{2}\left(\frac{du_l}{dt}\right)^2+V_{\rm sub}(u_l)+\frac{g}{2}(u_{l+1}-u_l)^2\right], \qquad (1)$$

where u_l is the displacement of the lth particle from its equilibrium position and g is the coupling constant between particles in the chain. We use a system of dimensionless units such that the particle's mass becomes equal to 1 and the period and amplitude of the substrate potential $V_{\rm sub}(u)$ are $a_s=2\pi$ and $\varepsilon_s=2$, respectively. The minimum of this potential is chosen as $V_{\rm sub}(0)=0$. For the classical FK model, the potential $V_{\rm sub}(u)$ is assumed to be of the simplest, sinusoidal form

$$V_{\rm sub}(u)=1-\cos u. \qquad (2)$$

The Hamiltonian (1) generates the equations of motion

$$\frac{d^2u_l}{dt^2}-g(u_{l+1}+u_{l-1}-2u_l)+V'_{\rm sub}(u_l)=0, \qquad (3)$$

where we define $V'_{\rm sub}(u)\equiv dV_{\rm sub}(u)/du$. Because of the topology of the potential $V_{\rm sub}(u)$, the system possesses degenerate ground states for which all particles occupy all minima of the potential and then the simplest excited state is *a kink* that connects two neighboring states. The kinks were introduced by Frenkel and Kontorova [1] to describe crystal dislocations. Their exact shape in a discrete FK chain is not known in an explicit analytical form because the discrete set of coupled nonlinear equations (3) cannot be solved analytically in a general case. From the physical point of view, a kink can be viewed as *a local defect* and therefore one may wonder how such defects affect the dynamical properties of the chain, in particular the spectrum of its small-amplitude excitations.

In the limit of strong coupling, i.e., when $g\gg 1$, an approximate solution can be obtained in the framework of the continuum approximation $l\to x=la_s$ and $u_l(t)\to u(x,t)$, so that Eq. (3) reduces to the partial differential equation (sometimes called the nonlinear Klein-Gordon equation)

$$\frac{\partial^2 u}{\partial t^2}-d^2a_s^2\frac{\partial^2 u}{\partial x^2}+V'_{\rm sub}(u)=0, \qquad (4)$$

where $d=\sqrt{g}$ defines the kink's width, in units of the period of the substrate potential. For the sinusoidal substrate potential (2), Eq. (4) becomes the well-known exactly integrable sine-Gordon (SG) equation [3]. Then, the kinks of the FK

model in the continuum limit are described by the soliton solutions of the SG equation and the spectrum of all linear modes around the kink can be found in an explicit form. It includes *a continuum frequency band* associated with nonlocalized propagating solutions (lattice phonons), modified by the presence of the kink. In addition, the small-amplitude excitation spectrum includes *the zero-frequency localized mode*, the so-called Goldstone mode, associated with the translational invariance of the SG model.

When the potential $V_{\rm sub}(u)$ deviates from the sinusoidal shape (2), the spectrum of the continuum model can be modified qualitatively by the appearance of additional localized modes, or *kink internal modes*, with frequencies below the lowest phonon frequency, i.e., in the gap of forbidden frequencies for phonon modes [4,5]. The existence of these localized modes has important consequences on the kink dynamics because they can temporarily store energy taken away from the kink's kinetic energy, which can later be restored again in the kinetic energy. This gives rise to *resonant structures* in kink-antikink collisions [5]. The similar effect is known for the kink-impurity interactions [6] where an impurity mode plays the role of the kink's internal mode.

For lattice models very little is known about the kink's internal modes. The only mode that has been investigated extensively so far is the translational mode, or the Goldstone mode, which is important because the kink breaks the translational invariance. In a discrete lattice, the frequency of this mode increases from zero (which corresponds to the continuum limit) as discreteness increases; this is associated with the existence of a potential barrier in a discrete lattice that must be overcome to move the kink along one lattice spacing [7]. This potential is known as the Peierls-Nabarro (PN) potential in the context of the dislocation theory. When the potential $V_{\rm sub}(u)$ deviates from the sinusoidal shape, new features appear. In particular, the PN barrier was found to oscillate as a function of the coupling parameter g (or the kink's width) [4]. These oscillating dependence corresponds to an exchange of stability between two positions of the kink in a lattice, one centered on a particle site and the other centered at the middle between two neighboring sites.

For other types of localized kink modes that may appear for some potential shapes, almost nothing is known about the role of discreteness; it is this aspect that we want to analyze in this paper. First of all, we would like to note that discreteness has a qualitative effect on the continuum spectrum of a lattice. While in the continuum model the phonon band extends to infinity in the direction of high frequencies, it is bounded from above for a discrete lattice due to the fact that there exists the minimum oscillation wavelength defined by the lattice spacing. The existence of an upper region forbidden for the propagating (or phonon) modes opens a new space for the existence of the kink's internal modes. We show in this paper that, in this domain, kink modes of the optical type, i.e., where adjacent particles move out of phase, may exist for some potential shapes. Finally, we go beyond the linear approximation for the kink's internal modes and study *nonlinear kink internal modes*. We show that, even in the case of a harmonic coupling between particles and for the sinusoidal potential, nonlinear kink internal mode can appear below or above the phonon band.

The paper is organized as follows. In Sec. II we present a general discussion of the kink's internal modes that allows us to understand the physics and some properties of this kind of localized excitation around the kink. Then, in Secs. III and IV we summarize our results for the cases of *weak* ($g \ll 1$) and *strong* ($g \gg 1$) interparticle interactions, respectively. Section V includes the analysis of the effect of nonlinearity on the kink's internal mode. Section VI concludes the paper.

II. KINK'S INTERNAL MODES: A QUALITATIVE PICTURE

A. Kink's internal modes as impurity modes

Before attempting a detailed analysis of the spectrum of a kink in a generalized FK model using analytical and numerical methods, it is useful to get a general feeling of the physics and results. This can be achieved by means of *qualitative approach* described in this section.

In the present paper we consider, for definiteness, the example of the generalized FK model with a nonsinusoidal substrate potential of the form

$$V_{\rm sub}(u)=\frac{(1-r)^2(1-\cos u)}{1+r^2+2r\,\cos u}. \tag{5}$$

This model of the substrate potential was introduced by Peyrard and Remoissenet [4], so that below we refer to the potential (5) as the Peyrard-Remoissenet (PR) potential. The shape of the potential is defined by the parameter r, $|r|<1$. For $r>0$ the potential (5) has flat bottoms separated by thin barriers, while for $r<0$ it has the shape of sharp wells separated by flat wide barriers. For small values of r, the potential reduces to the double-sine-Gordon (DSG) potential [8]

$$V_{\rm sub}(u)\propto -\cos u + r\,\cos(2u). \tag{6}$$

When the particle displacements are small, i.e., for $|u_l| \ll a_s$, we can apply the harmonic approximation replacing $V_{\rm sub}(u)$ by its truncated Taylor series $V_{\rm sub}(u)\approx \frac{1}{2}V''_{\rm sub}(0)u^2$. The solutions of the equations of motion are then plane waves or *phonons*, $u_l(t) \propto \exp\{i\omega_{\rm ph}(\kappa)t - i\kappa l\}$, with the spectrum defined as

$$\omega^2_{\rm ph}(\kappa)=\omega^2_{\rm min}+2g(1-\cos\kappa), \quad \omega^2_{\rm min}=\frac{(1-r)^2}{(1+r)^2}, \tag{7}$$

κ being the dimensionless wave number, $|\kappa|\leq\pi$. The linear spectrum (7) of the discrete FK model is bounded from above as well as from below and it occupies the region $\omega_{\rm min}\leq\omega\leq\omega_{\rm max}$, where

$$\omega_{\rm min}\equiv\omega_{\rm ph}(0)=\sqrt{V''_{\rm sub}(0)}=\frac{(1-r)}{(1+r)},$$

$$\omega_{\rm max}\equiv\omega_{\rm ph}(\pi)=\sqrt{\omega^2_{\rm min}+4g}.$$

In order to understand how a kink can modify the phonon spectrum of linear modes in the lattice, first we recall the effects produced by *a localized impurity* in a harmonic lattice. Let us consider *an isotopic impurity*, such that the mass m_0 of one of the lattice particles, e.g., that with the number

$n=0$, differs from all other masses, $m=1$. In the absence of the interatomic coupling (i.e., at $g=0$), the impurity oscillates with the frequency $\omega_{\rm imp}^{(0)}=\sqrt{V''_{\rm sub}(0)/m_0}$, which is different from the frequency of the lattice particles (which in the case of a lattice coincides with the minimum edge of the phonon band) $\omega_{\rm min}$. The impurity frequency is larger for the case of a light-mass impurity $m_0<m$ and smaller in the case of a heavy-mass impurity $m_0>m$. Including the interatomic interaction $g\neq 0$, we find that the impurity frequency gets shifted $\omega_{\rm imp}^{(0)}\rightarrow\omega_{\rm imp}=\omega_{\rm imp}^{(0)}+\Delta\omega$, where $\Delta\omega$ has the sign of the mass difference $\Delta m=m_0-m$. If the impurity frequency lies within the phonon spectrum band, i.e., $\omega_{\rm min}\leqslant\omega_{\rm imp}\leqslant\omega_{\rm max}$, the corresponding impurity-induced mode is called *a virtual mode*, or *quasimode*. Otherwise, when $\omega_{\rm imp}<\omega_{\rm min}$ or $\omega_{\rm imp}>\omega_{\rm max}$, the impurity mode becomes *a local mode* and oscillations near the impurity decay exponentially. The local mode has an infinite lifetime in a harmonic approximation [9–11].

Introducing an impurity into a lattice always leads to the creation of one impurity mode, either a virtual mode, for a weak perturbation of the chain, or a local mode, for stronger perturbations. Because a change of one of the lattice masses does not change the total number of the degrees of freedom, the degree of freedom associated with the impurity mode must appear from one of the phonon modes of the harmonic lattice. In the case of a local mode, the localized eigenmode can split from the bottom of the phonon spectrum band in the case $m_0>m$ or from the top of the phonon spectrum band for $m_0<m$. Similarly, a lattice with N impurities should have N impurity modes, but only some of them may correspond to spatially localized modes.

Now, let us consider the FK chain without impurities but with a single kink. The kink (or antikink) corresponds to a topologically stable local compression (or expansion) of the chain, so that it is an extended object with a width $d=\sqrt{g}$. Clearly, near the kink's core the lattice is in a perturbed state and the number of the corresponding ''perturbed particles'' M is proportional to the kink's width $M\sim d=\sqrt{g}$. Thus we can expect the existence of M internal kink modes (similar to the impurity modes in a lattice with defects), either virtual or local. The lowest frequency ω_1 corresponds to the mode where particles oscillate in phase, while the highest frequency ω_M corresponds to the out-of-phase particle oscillations. Because the kink's core should include *at least two particles* $M\geqslant 2$, this simple reasoning suggests that we can always expect the existence of at least two internal kink modes. The mode with the lowest frequency corresponds to oscillations of the kink as a whole in a potential well created by the PN potential [12,13] with the PN frequency $\omega_1=\omega_{\rm PN}$. This mode reduces to the well-known Goldstone mode with $\omega_1=0$ in the continuum limit, i.e., when $g\gg 1$. For the SG model, the frequency of the second internal kink mode ω_2 coincides with the minimum frequency of the phonon spectrum band $\omega_2=\omega_{\rm min}$. Because the density of the phonon states of a harmonic lattice tends to infinity at the phonon spectrum edges (see, e.g., [10]), the second mode of the SG kink is delocalized and therefore it cannot be observed. But for a nonsinusoidal substrate potential, such as the PR potential (5) or the DSG potential (6), the second mode exists as a local mode for $r<0$ or as a virtual mode for $r>0$. Moreover, for the PR substrate potential (5) the number of local internal kink modes increases with an increase of the value $|r|$ for $r<0$ [5]. Note that the low-frequency localized modes (except the first one called the PN mode) are known as the kink's shape modes first observed for the ϕ^4 model (see, e.g., Ref. [5]). The kink's shape mode with the frequency ω_2 has the simple physical interpretation for the DSG potential (6) at $r<-\frac{1}{4}$, when the usual kink (2π kink) can be regarded as that consisting of two coupled π subkinks [5,14–16]. Such a kink can be interpreted as a ''molecule'' consisting of two ''atoms'' (π subkinks) and the ω_2 mode corresponds to relative oscillations of these atoms.

B. Effect of discreteness and shape of potential

In this subsection we discuss the qualitative features of the kink oscillations and the property of kink's internal modes in a discrete lattice. As is already understood (see [7,17,18]), discreteness decreases the kink's effective width and therefore one can expect that it will increase the frequency of the kink's internal mode. This is the case of the zero-frequency Goldstone mode of the continuum model, which in a discrete lattice becomes the nonzero PN mode $0<\omega_1=\omega_{\rm PN}<\omega_{\rm min}$. However, the results presented below show that the simple qualitative argument connecting the kink's width and the frequencies of low-frequency local modes (kink's internal modes) is not always valid and we display some interesting unexpected features even for the simplest case of the sinusoidal substrate potential.

Another important feature of any discrete model is the existence of the upper cutoff frequency of the phonon band $\omega_{\rm max}<\infty$. As a result, one can expect not only low-frequency (LF) kink internal modes, but also high-frequency (HF) modes with the frequencies above the maximum frequency of the phonon band, $\omega_{\rm max}$. We show below that this is indeed the case for some shapes of the substrate potential and we describe these localized modes analytically, in the cases of weak and strong interatomic coupling.

When the amplitude of kink oscillations increases, we should take into account nonlinear (or anharmonic) effects. For impurity modes nonlinear effects lead to a decrease of the frequency of the LF impurity mode and, correspondingly, to an increase of the frequency of the HF mode, provided the oscillation amplitude grows [11]. This effect was analyzed in detail for the lowest PN mode by Boesch *et al.* [19]. Namely, an increase of the amplitude of the kink's oscillations at the bottom of the PN potential leads to a decrease of the frequency from the value $\omega_1(0)=\omega_{\rm PN}$ to zero, at some critical value. A decrease of the frequency was also observed for the shape mode ω_2 in the DSG model for $r<-\frac{1}{4}$, when the 2π kink can be interpreted as that consisting of two coupled π subkinks [14–16].

Figures 1(a), 1(b), 2(a), and 2(b) show some examples of the linear spectrum of kink excitations in the generalized FK model with the PR potential (5), calculated numerically. To obtain these results, first we determine the static configuration of particles, corresponding to a kink, by minimizing the energy of the chain with the corresponding boundary conditions. When all the equilibrium positions $u_l^{\rm eq}$ of the particles in a chain with a kink become known, we study the spectrum of small-amplitude oscillations around this state by looking

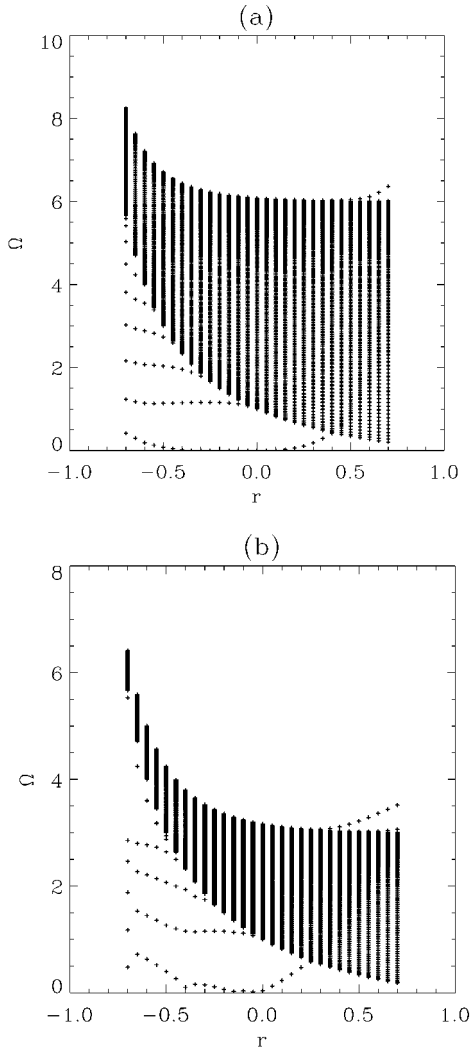

FIG. 1. Spectrum of small-amplitude excitations around a kink in the generalized FK model as a function of the parameter r determining the shape of the potential ($r=0$ gives a sinusoidal potential) for two values of the discreteness parameter d: (a) $d=3.0$ and (b) $d=1.5$.

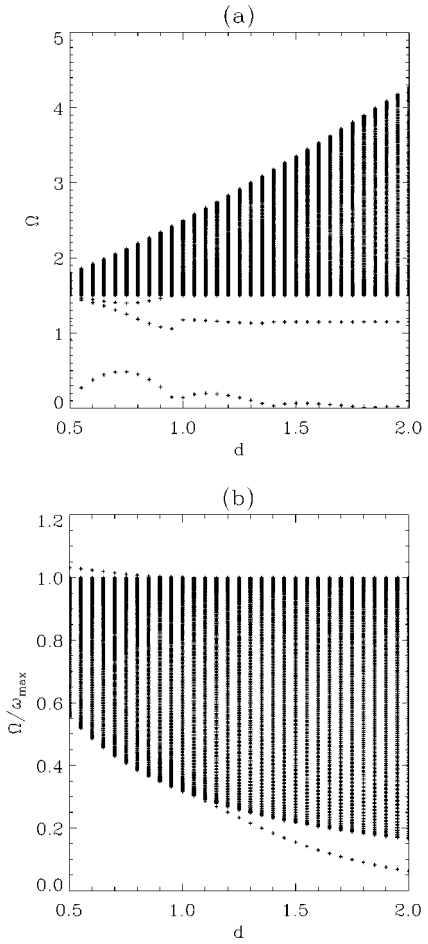

FIG. 2. Spectrum of small-amplitude excitations around a kink in the generalized FK model as a function of the discreteness parameter d for two values of the parameter r determining the shape of the potential. Since d is a measure of the kink's width, high discreteness corresponds to small values of d. (a) $r=-0.2$ and (b) $r=+0.2$. In this latter case, the frequencies have been divided by $\omega_{\max}$ to show more clearly the existence of a mode above the top of the phonon band for small d.

for a solution in the form $u_l=u_l^{\rm eq}+v_l e^{i\omega t}$. We assume that the perturbation v_l is sufficiently small ($v_l \ll a$) and ignore all nonlinear terms in the equations of motion for v_l. Introducing this ansatz into Eq. (3), we obtain a system of linear equations that can be written in a matrix form $\mathbf{Bv}=\omega^2\mathbf{v}$, with $\mathbf{v}\equiv\{v_l\}$, where a triagonal matrix $\mathbf{B}$ is the dynamical matrix of the lattice in the presence of a kink and $B(l,l)=2g+V''_{\rm sub}(u_l^{\rm eq})$, $B(l,l\pm1)=-g$. This matrix is diagonalized numerically for a chain of N particles with fixed ends. The value of N is chosen large enough to avoid perturbations due to boundary effects (typically $N=200$, but it has been extended to 600 for broader kinks and larger values of d). Its eigenvalues give the frequencies of the small-amplitude oscillations around the kink and the corresponding eigenvectors describe the spatial profile of each mode.

Figure 3(a) shows one example of the spectrum of a discrete kink at $r=-0.05$ and $d=\sqrt{g}=0.8$. The kink shape is shown in Fig. 3(b). We notice that the kink contains very few particles and that its center is situated between two particles. This configuration will be henceforth denoted by a ''noncentered'' kink. Such a position of the kink corresponds to the minimum energy for the standard FK model (sinusoidal potential). As we have chosen a fairly discrete case, the spectrum presented in Fig. 3(a) includes the PN mode with the frequency $\omega_{\rm PN}=\omega_1=0.2482$, which is a significant part of $\omega_{\min}=(1-r)/(1+r)=1.1053$, indicating that this kink is pinned by the lattice discreteness. Figure 3(c) shows the eigenvector associated with this localized mode. It has the shape of the derivative of the kink profile function, which is not surprising for a mode that will tend to the Goldstone mode in the continuum limit (large d). The spectrum of Fig. 3(a) shows also the presence of the second mode, which is isolated below the continuum band. This is the kink's internal mode with the frequency $\omega_2=1.0229$. Its eigenvector is shown in Fig. 3(d). Figures 3(e) and 3(f) show the eigenvectors of the mode at the bottom of the phonon band and the mode at the top of the band, respectively. As expected for modes that belong to the phonon spectrum, they are not localized and extend over the whole atomic chain. These phonon modes are modified by the presence of the kink. This is

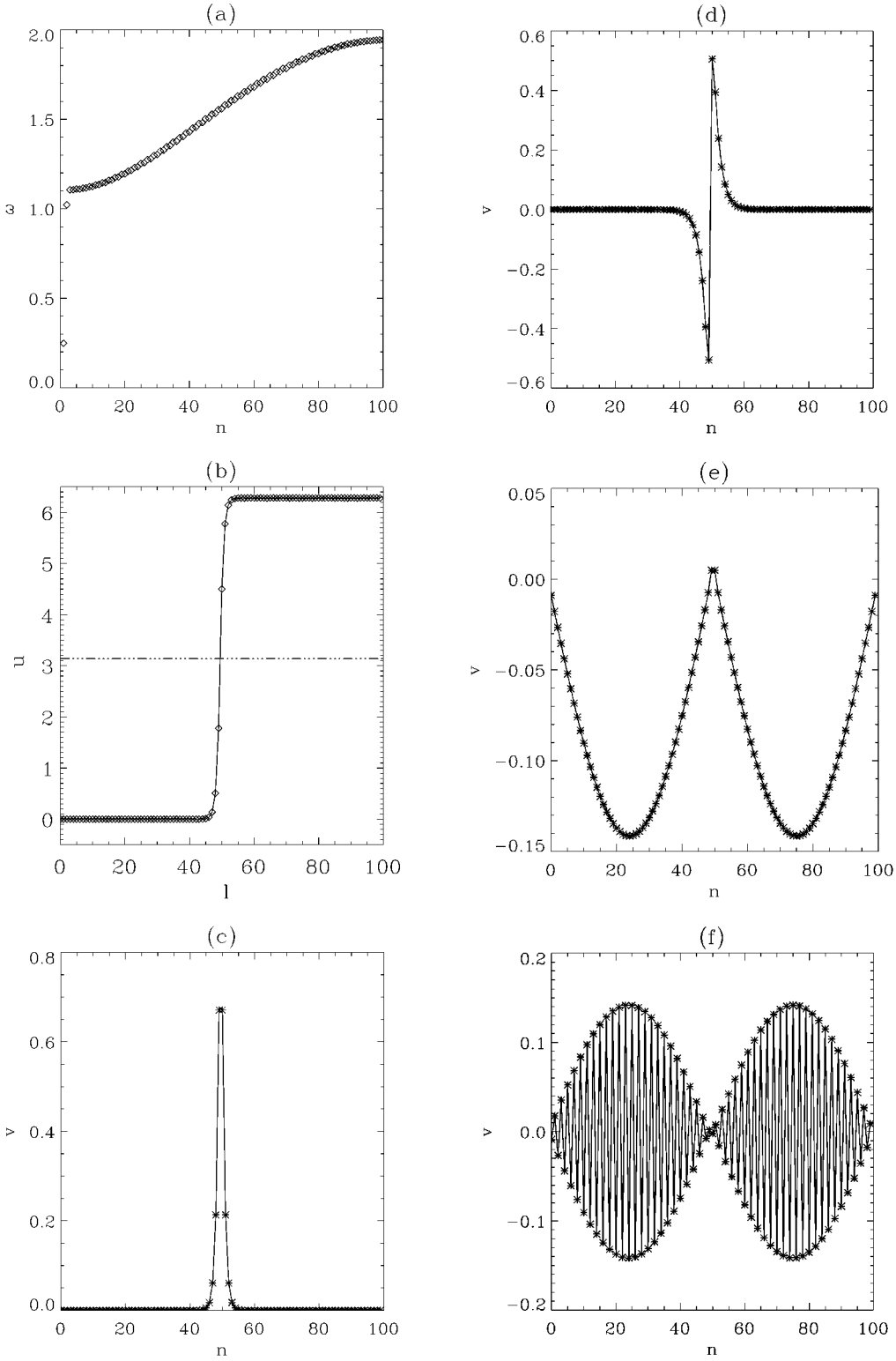

FIG. 3. Example of the spectrum of a discrete kink in the generalized FK model. The results are shown for $N=100$ for clarity. Shown are (a) eigenfrequencies of the small-amplitude excitations around the kink, (b) the shape of the static kink, (c) the eigenvector of the lowest mode (this is the PN mode that would give the Goldstone mode in the continuum limit), (d) the eigenvector of the second mode (this is a localized shape mode of the kink), (e) the eigenvector of the third mode (this mode is the lowest nonlocalized mode that belongs to the continuous spectrum band), and (f) the eigenvector of the highest nonlocalized mode of the continuous spectrum band.

known for the spectrum of the SG model and is also true for a discrete model.

Figures 1(a), 1(b), 2(a), and 2(b) illustrate the general features of the kink's linear spectra discussed above. Let us consider first the results presented in Fig. 1(a). The phonon band appears clearly, although it does not look continuous because the calculations have been performed with only 200 particles so that the phonon band can contain at most 200

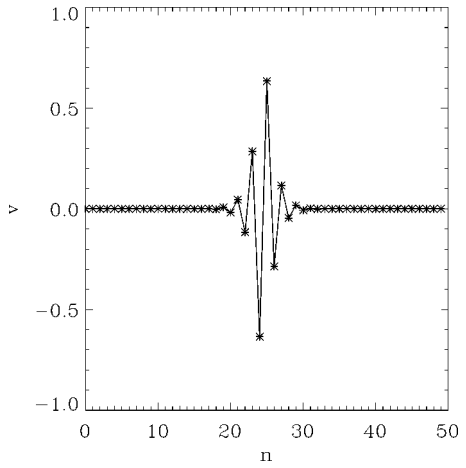

FIG. 4. Eigenvector of a kink's high-frequency internal mode for $r=0.6$ and $d=1.5$. The frequency of this mode is $\omega=3.3620$, while the top of the phonon band is situated at $\omega_{\max}=3.0732$. Neighboring particles move out of phase, contrary to the kink's low-frequency internal mode.

points. The bottom of the band is determined by the lower cutoff frequency $\omega_{\min}=(1-r)/(1+r)$ and therefore it varies with r. The top of the band is defined as $\omega_{\max}=(\omega_{\min}^2+4d^2)^{1/2}$. For $r=0$, we do not see clearly the PN mode in Fig. 1(a) because its frequency is almost equal to 0 for the value $d=3$ that was used to generate this figure (for $d=3$ the properties of the FK model are already very close to those of the SG model). The frequency of the PN mode increases as r deviates from 0, especially for $r>0$ [4]. In the low-frequency range, below the phonon band, Fig. 1(a) shows the successive appearance of localized modes as r decreases toward the limit value $r=-1$ (see Ref. [5]). These modes emerge from the phonon band because, as discussed above, they originate from the modification of phonon spectrum. Looking at the region of large r, one can see also the appearance of localized modes *above* the phonon band, as predicted by our discussions. Figure 4 presents one example of the eigenvector of such a HF localized mode. It shows that the particles move out of phase as expected for a mode that evolved from a phonon mode situated at the edge of the phonon band.

Figure 1(b) presents similar results for a more discrete case, $d=1.5$. The HF localized modes, which are a special feature of discrete models since they do not exist in the continuum limit, are more visible and the figure shows that, as for the LF modes, a discrete kink can have several HF localized modes. In addition, in Fig. 1(b) one notices that the PN mode and the LF localized modes for $r<0$ show a nonmonotonic variation with r [or d, in Fig. 2(a)]. This effect is associated with a change of the stable position of the kink with respect to the lattice sites as r or d evolve. The kink's stable position can be either noncentered, as shown in Fig. 3(a), or centered when the kink's center is exactly at a particle site. A transition between these two states is known to induce oscillations of the PN barrier [4], but our results show that this phenomenon affects the whole spectrum of the kink's localized modes.

Another interesting feature that appears in Figs. 1(a) and 1(b) is that, for large r, the PN mode *penetrates into the continuum part of the spectrum*. Therefore, such a kink does not have a localized translational mode. An analysis of the phonon band in this case shows that the former PN mode appears as a maximum of the density of phonon states along the prolongation of the curve showing the variation of the PN frequency versus r for lower values of the shape parameter r. This ''track'' of the PN mode in the continuum spectrum is also visible on the eigenfunctions of the modes that have a frequency close to it. The even modes, i.e., the modes having the same symmetry as the PN mode, have the maximum amplitude around the kink's center, which is reminiscent of the shape of a localized PN mode superimposed on a nonlocalized mode. The odd-symmetry mode, or the mode far from the track, does not exhibit such a maximum. The absence of a localized translational mode can also be tested by driving the motion of the kink by a uniform external field. We did not succeed in driving the kink at low speed. When the applied field exceeds a depinning threshold, the kink starts moving fast and its motion is accompanied by a very strong growing tail of radiation. This effect can be understood if one treats the track of the PN mode in the phonon band as a *nonlocalized translational mode*.

Figures 2(a) and 2(b) show the deformation of the kink's spectrum for varying discreteness parameter d. Besides the change of the phonon band, one sees clearly from these figures the growth of the frequency of the PN mode when discreteness increases. In addition, Fig. 2(b) shows how discreteness induces the formation of HF localized modes for $r>0$. Discreteness has also more subtle effects, not visible on the figures, which will be discussed below.

The qualitative discussion and numerical results have presented the main results of the role of discreteness and potential shape on the kink's spectrum in a generalized FK chain. This sets the stage for some analytical studies that are able to explain the origin of these results in some limiting cases and additional numerical results to exhibit some fine points.

III. WEAK-COUPLING CASE

A. Analytical results

First, we discuss the simplest case of a weak interaction between particles, i.e., $g\ll 1$, when the kink's core consists of two particles $M=2$. In the lowest-order approximation, we assume that all particles lie at the bottom of the corresponding wells of the substrate potential, while two particles (say, with the numbers $n=0$ and $n=1$) are shifted from the bottom in such a way that they create a kink describing a transition between two neighboring ground states of the chain. Under this assumption, we look for a static configuration of the particles in the form

$$u_l^{\text{kink}}\approx\begin{cases}0 & \text{for } l\leqslant -1\\ -b & \text{for } l=0\\ -a_s+b & \text{for } l=1\\ -a_s & \text{for } l\geqslant 2\end{cases} \tag{8}$$

and, using the motion equation (3), obtain an equation for the shift b, $g(a_s-3b)=V'_{\text{sub}}(b)\approx\omega_{\min}^2 b$, which has the solution

$$b\approx\frac{a_s g}{\omega_{\min}^2+3g}.$$

Because $M=2$, we expect the existence of at least two internal kink modes. To find these modes and the corresponding frequencies, we substitute the function $u_l(t)=u_l^{\rm kink}+\delta u_l(t)$, $\delta u_l \propto e^{i\omega t}$, into Eq. (3) and then linearize it with respect to small oscillations $\delta u_l(t)$, thus obtaining an equation for eigenfrequencies ω_i, $i=1,2$. To find the frequencies in an explicit form, we introduce the Green's function (see, e.g., Ref. [11])

$$G(l,l';\omega)=-i\lim_{\delta\to 0}\int_{-\infty}^{+\infty}dt\; e^{i\omega t-\delta|t|}\langle \hat{T}\hat{u}_l(t)\hat{u}_{l'}(0)\rangle,$$

where $\hat{T}$ is the time-ordering operator, $\hat{u}_l(t)$ is the displacement operator in the Heisenberg representation, and $\langle\,\rangle$ means an average over the ground state. The matrix function $\mathbf{G}(\omega)\equiv G(l,l';\omega)$ satisfies the matrix equation $(\omega^2\mathbf{I}-\mathbf{B})\mathbf{G}(\omega)=\mathbf{I}$, where $\mathbf{I}$ is the unit matrix and $\mathbf{B}$ is the matrix with the elements

$$B(l,l')=\left(\frac{\partial^2 H}{\partial u_l \partial u_{l'}}\right)_{u_l=u_l^{\rm kink}}. \tag{9}$$

In our case the matrix $\mathbf{B}$ can be presented in the form $\mathbf{B}=\mathbf{B}_0+\delta\mathbf{B}$, where $\mathbf{B}_0$ is the ''unperturbed'' matrix describing linear oscillations of the chain without the kink,

$$B_0(l,l')=\delta_{l,l'}(\omega_{\rm min}^2+2g)-(\delta_{l,l'+1}+\delta_{l,l'-1})g,$$

while the perturbation $\delta\mathbf{B}$ is caused by the presence of a kink

$$\delta B(l,l')=\delta_{l,l'}(\delta_{l,0}+\delta_{l,1})[V''_{\rm sub}(b)-\omega_{\rm min}^2]$$

$$\approx\frac{1}{2}\delta_{l,l'}(\delta_{l,0}+\delta_{l,1})V''''_{\rm sub}(0)b^2.$$

The Green's function $\mathbf{G}$ satisfies the Dyson-type equation

$$\mathbf{G}=\mathbf{G}_0+\mathbf{G}_0\delta\mathbf{B}\mathbf{G}, \tag{10}$$

where $\mathbf{G}_0$ is the Green's function of the FK chain. It satisfies the equation $(\omega^2\mathbf{I}-\mathbf{B}_0)\mathbf{G}_0(\omega)=\mathbf{I}$ and has the form $G_0(l,l';\omega)=D_{l-l'}(z)$, where

$$D_l(z)=A(z)y^{|l|}(z), \tag{11}$$

$$A(z)=-\frac{i}{2g\sqrt{1-z^2}}. \tag{12}$$

Here we have introduced two new variables y and z according to the relations

$$y(z)=-z+i\sqrt{1-z^2},\quad z=(\omega^2-\omega_{\rm mid}^2)/2g, \tag{13}$$

where $\omega_{\rm mid}$ is the center of the phonon band $\omega_{\rm mid}^2=\omega_{\rm min}^2+2g$. For the frequencies within the phonon band $\omega_{\rm min}\leqslant\omega\leqslant\omega_{\rm max}$, we have $|z|\leqslant 1$. Outside the phonon band, where $|z|>1$, the square root in Eqs. (12) and (13) should be calculated as

$$\sqrt{1-z^2}=-i\;{\rm sgn}(z)\sqrt{z^2-1}. \tag{14}$$

Equation (10) can be easily solved; its solution gives the expression for the function $G(0,0;\omega)$,

$$G(0,0;\omega)=\left\{D_0(z)+\frac{\delta B(0,0)}{g}D_1(z)\right\}Z^{-1}, \tag{15}$$

where

$$Z=1-2\,\delta B(0,0)D_0(z)-\frac{\delta B^2(0,0)}{g}D_1(z). \tag{16}$$

Analogously, we can determine other elements of the matrix $\mathbf{G}$, all of them having the same denominator Z.

Zeros of the equation $Z=0$ determine the poles of the Green's function and therefore the frequencies of kink's internal modes. Using Eqs. (11)–(14) and (16), the equation $Z=0$ can be rewritten as

$$(2g^2-\gamma^2)\sqrt{z^2-1}=\gamma\;{\rm sgn}(z)(2g-\gamma z), \tag{17}$$

where $\gamma\equiv\delta B(0,0)\approx\frac{1}{2}V''''_{\rm sub}(0)b^2$. The solution of Eq. (17) is defined as

$$z_{\rm PN}=-\left[1+\frac{\gamma^2}{2g(g-\gamma)}\right] \tag{18}$$

and corresponds to a local mode provided $z_{\rm PN}<-1$ (or $\gamma<g$). However, the direct substitution of the solution (18) into Eq. (17) shows that the latter is satisfied only provided $\gamma<0$. For the PR substrate potential (5) we have

$$V''''_{\rm sub}(0)=-\omega_{\rm min}^2\frac{1-10r+r^2}{(1+r)^2} \tag{19}$$

and the condition $\gamma<0$ leads to the inequality $r>r_0$, where $r_0=5-2\sqrt{6}\approx 0.101$. Furthermore, the condition $\omega^2>0$ leads to the additional inequality

$$\gamma>\gamma_0\equiv-\frac{1}{2}\omega_{\rm min}^2(1+\sqrt{1+4g/\omega_{\rm min}^2}) \tag{20}$$

because at $\gamma=\gamma_0$ the PN frequency vanishes.

Thus the kink's LF internal mode exists provided both the inequalities $r<r_0$ and $\gamma>\gamma_0$ are satisfied simultaneously; this mode corresponds to the PN mode with the frequency

$$\omega_{\rm PN}=\left\{\omega_{\rm min}^2-\frac{\gamma^2}{g-\gamma}\right\}^{1/2}. \tag{21}$$

The second solution of the equation $Z=0$ can be found as

$$z_{\rm HF}=1+\frac{\gamma^2}{2g(g+\gamma)} \tag{22}$$

and corresponds to a local mode provided $z_{\rm PN}>1$ (or $\gamma>-g$). Again, a direct substitution of the solution (22) into Eq. (16) shows that the equation is satisfied only for $\gamma>0$ (or $r>r_0$). This HF mode corresponds to the antiphase vibrations of two atoms of the kink's core with the frequency

$$\omega_{\rm HF}=\left\{\omega_{\rm max}^2+\frac{\gamma^2}{g+\gamma}\right\}^{1/2}. \tag{23}$$

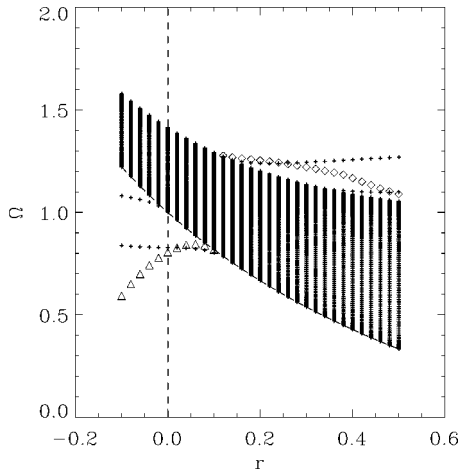

FIG. 5. Spectrum of the FK chain containing a very discrete kink ($d=0.5$, corresponding to $g=0.25$) as a function of the shape parameter r. The crosses are the frequencies of the linear modes around the kinks, determined numerically. The triangles and diamonds indicate, respectively, the frequencies of the PN mode and the kink's high-frequency internal mode, calculated analytically in the weak-coupling limit.

Thus, in the weak-coupling limit, depending on the shape of the substrate potential, a discrete kink has either the PN mode if $r<r_0$ or the HF localized mode, if $r>r_0$.

B. Comparison with numerical results

The analytical results presented above confirm the numerical observations reported in Sec. II, i.e., that for large r and sufficiently strong discreteness the PN mode may disappear by penetrating into the phonon band. For a more detailed verification of the validity of the analytical approach in the weak-coupling limit, we have determined numerically the spectrum of a very discrete kink (i.e., $d=0.5$, so that $g=0.25$) as a function of r. In Fig. 5 the numerical results are compared with the analytical calculations obtained above for the weak-coupling limit. The theoretical values of ω_{PN} and ω_{HF} have been found from Eqs. (21) and (23), respectively. The values of b, entering in the expression for γ, have been taken from the numerical static kink solution. In the range $0\leqslant r\leqslant 0.2$, the analytical predictions of the domain of existence and frequencies of the PN and HF modes are *very accurate*. This is rather remarkable when one considers that an accurate determination of the PN frequency of the SG kink ($r=0$) was only obtained through elaborate analytical methods [20]. The success of our analytical approach is explained by the fact that it treats the lattice discreteness intrinsically. But one cannot expect the results to give a good agreement when the kink's core contains more than two particles. This is the case of strong coupling, but also large values, of the parameter r, because the deformation of the potential is associated, for positive r, with a broadening of the kink's core [4]. Figure 5 shows that for large r the analytical prediction of ω_{HF} deviates from the numerical results. The second HF mode that appears at large r is the consequence of an increase of the number of particles in the kink core, as discussed in Sec. II. The analytical result obtained in the weak-coupling limit shifts gradually from the first HF mode to the second mode, which appears at larger r, because the analytical calculation determines the mode that is the closest to the phonon band and therefore it is not appropriate to follow the frequency of the mode versus r when several local modes exist. For negative r, the kink stays sharp, with only two particles in the core, but its properties cannot be described accurately by the simple analytical approach because, in particular, the position of the kink's center between two particles may not be a stable position [4].

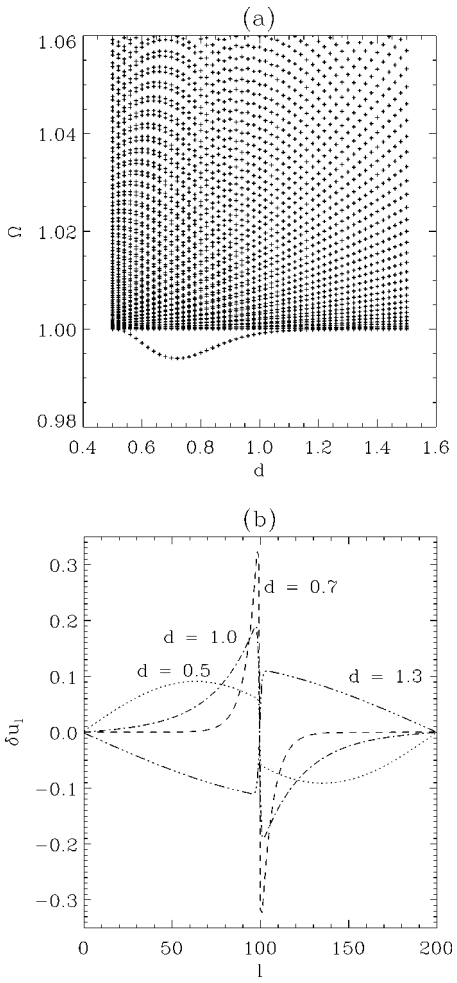

FIG. 6. Spectrum of a discrete SG kink. (a) Magnification of the bottom of the phonon band for $0.5\leqslant d\leqslant 1.5$. The frequencies of the linearized modes around the kink have been calculated for a chain of 400 particles, with fixed boundary conditions. (b) Shape of the lowest mode of odd frequency (the mode with lowest frequency in the spectrum is the even translational mode) for several values of d showing the shift from the nonlocalized to the localized state in a small range of d values.

C. Kink's internal modes in the discrete SG chain

The effect of discreteness on the spectrum of the kink's internal modes is particularly interesting for the sinusoidal potential ($r=0$) because, in the continuum limit, this model is described by the integrable SG equation where a kink has only one localized mode, the Goldstone mode associated with the kink's translation. Figure 6(a) shows a magnification of the spectrum around the bottom of the phonon band for the discreteness parameter d in the region $0.5\leqslant d\leqslant 1.5$.

One can see that for small d ($0.52<d<1.26$) one mode becomes shifted outside the phonon band and then it returns to the phonon band for higher values of d. This means that the discrete SG kink can possess a localized internal mode in addition to the translational mode. Figure 6(b) shows the shape of the corresponding eigenmode, which is the odd mode corresponding to the lowest frequency. For $d=0.5$ or 1.3, it has the characteristic shape of a nonlocalized mode and corresponds approximately to one period of a sinusoidal function, slightly distorted and with a large phase shift due to the presence of the kink. To understand this shape, one must keep in mind that the numerical results are obtained for a finite chain with fixed boundary conditions. Therefore, we cannot observe the true bottom of the band that would correspond to a mode with an infinite wavelength. The calculations have been performed with chains of 200 and 400 sites to check that the results are not perturbed by finite-size effects. On the contrary, for $d=0.7$ or $d=1$, which correspond to a mode below the bottom of the phonon band, the eigenfunction shows an exponential decay away from the center. The decay is faster for $d=0.7$ because in this case the mode is farther away from the edge of the phonon band, as can be seen in Fig. 6(a). The curvature of the eigenfunction (downward for a nonlocalized mode and upward for a localized mode) is a sensitive test of localization because it shows a qualitative change from the localized and the nonlocalized mode. The existence of an extra localized mode in a narrow range of the discreteness parameter d is also observed for other potential shapes close to the sinusoidal shape (e.g., $r=-0.01$), but the case of the discrete SG kink is perhaps the most interesting because the spectrum is known exactly in the continuum limit. It indicates that discreetness can change the modes around a kink *qualitatively* and create a kink-shape mode, even for harmonic interactions and a perfectly sinusoidal potential.

IV. STRONG-COUPLING CASE

A. General analysis

In the opposite case, when the interatomic coupling is strong, i.e., for $g\gg 1$, we can use the continuum approximation. In this case the shape of the static kink is determined, according to Eq. (4), by the equation $d^2u/dx^2=V'_{\rm sub}(u)$, or

$$\frac{du}{dx}=-\frac{\sigma}{d}\sqrt{2V_{\rm sub}(u)}, \tag{24}$$

where $\sigma=\pm 1$ is the kink's topological charge. Equation (24) can be solved explicitly only for some special cases. For example, for the sinusoidal substrate potential the kink shape is given by the expression (recall $a_s=2\pi$)

$$u_k^{\rm SG}(x)=4\tan^{-1}\exp\left\{-\sigma\frac{(x-X)}{d}\right\}, \tag{25}$$

where X is the coordinate of the kink's center. Although for a general form of the substrate potential the shape of the kink can be found only in an implicit form, we can obtain an approximate analytical result useful for the subsequent analysis of the kink's internal modes. Indeed, in the region of the kink's core, $|x-X|<d$, the kink's shape can be presented as the Taylor expansion

$$u^{\rm kink}(x)=u(X)+u'(X)(x-X)+\frac{1}{3!}u'''(X)(x-X)^3+\cdots, \tag{26}$$

where $u(X)=-\sigma a_s/2=-\pi\sigma$ and, according to Eq. (24), we have $u'(X)=-\sigma\sqrt{2V_{\rm sub}(\pi)}/d=-2\sigma/d$, $u'''(X)=u'(X)V''_{\rm sub}(\pi)/d^2=2\sigma\tilde{\omega}^2_{\rm min}/d^3$, and a similar expressions for higher-order derivatives. Here we have introduced the notation $\tilde{\omega}^2_{\rm min}=-V''_{\rm sub}(\pi)$ and have taken into account that $V_{\rm sub}(\pi)=\varepsilon_s=2$. Now, using this expansion we can define the effective kink width $d_{\rm eff}$ as $d_{\rm eff}=d/\sqrt{-V''_{\rm sub}(x_m)}=d/\tilde{\omega}_{\rm min}$. As particular cases, for the SG model we have $d_{\rm eff}=d$, while for the FK model with the PR potential (5) we obtain

$$d_{\rm eff}=\frac{1-r}{1+r}d=\omega_{\rm min}d, \tag{27}$$

i.e., $d_{\rm eff}>d$ for the case $r<0$ and $d_{\rm eff}<d$ for the case $r>0$.

Now, to find the kink's internal modes, we should look for a solution of Eq. (3) in the form

$$u_l(t)=u^{\rm kink}(la_s)+\delta u_l e^{i\omega t}, \tag{28}$$

where the amplitudes δu_l of kink-shape oscillations are assumed to be small. Further analysis of the kink's internal modes is different for the LF and HF modes and should be carried out separately.

B. Kink's low-frequency internal modes

For LF kink's internal modes, the particles near the kink's core oscillate approximately in phase. Therefore, we can use a standard continuum limit approximation by letting $\delta u_l\to\delta u(x)$ in Eq. (28) and assuming that $\delta u(x)$ is a slowly varying function of the particle number. Then, substituting Eq. (28) into Eq. (3) and expanding $V'_{\rm sub}(u)$ into the Taylor series with respect to a small deviation δu, we obtain the stationary pseudo-Schrödinger equation (see, e.g., Ref. [21])

$$\left[-\frac{d^2}{dx^2}+V_{\rm Sch}(x)\right]\delta u(x)=E\,\delta u(x), \tag{29}$$

where

$$V_{\rm Sch}(x)=d^{-2}\{V''_{\rm sub}[u^{\rm kink}(x)]-V''_{\rm sub}(0)\}, \tag{30}$$

so that $V_{\rm Sch}(x)\to 0$ when $|x|\to\infty$, and

$$E=d^{-2}(\omega^2-\omega^2_{\rm min}). \tag{31}$$

The potential $V_{\rm Sch}(x)$ has a width $d_{\rm eff}$, given by Eq. (27), and the depth V_0 given by the expression

$$V_0=\frac{1}{d^2}(\omega^2_{\rm min}+\tilde{\omega}^2_{\rm min})=\frac{2}{d^2}\,\frac{1+r^2}{1-r^2}. \tag{32}$$

The kink's internal modes correspond to localized eigenstates of Eq. (29) with negative eigenvalues. As is well known, in the one-dimensional Schrödinger equation with a

potential vanishing at infinity, there exists at least one localized eigenstate provided the area integral calculated for this potential is negative. This is indeed the case of the PR potential at small r and it is easy to check that the lowest discrete eigenvalue of the eigenvalue problem (29) is equal to $E_1=-(\omega_{\min}/d)^2$ with the eigenfunction $\delta u_1(x) \propto d[u^{\rm kink}(x)]/dx$. This solution corresponds to the Goldstone mode and describes the continuous translation of the kink in the continuum model. However, as will be seen below, for rather large d we observe that the PN mode tends to disappear, merging with the phonon band for large values of r. Thus the existence of a PN mode for any r, which one could expect from the existence of a Goldstone mode, is true only for d really large, i.e., for a nearly continuum limit.

Higher-order eigenvalues of the problem (29) can be found only numerically. In order to investigate them qualitatively, we consider the modified Pöschl-Teller (PT) potential

$$V_{\rm PT}(x)=-\frac{V_0}{\cosh^2(x/b)}, \tag{33}$$

which describes a potential well of the depth V_0 and width b and allows exact solutions [22]. Namely, it is known that there exist $N_{\rm PT}$ bound states for the potential well (33), where $N_{\rm PT}=\text{int}(\lambda)$ and $\lambda=\frac{1}{2}(1+\sqrt{1+4C})$, $C=V_0b^2$. The eigenvalues of the discrete eigenstates (bound modes) are found to be $E_i=-V_0(\lambda-i)^2/C$, where $i=1,2,,\ldots,N_{\rm PT}$. We notice that the number of the bound states as well as their eigenvalues are expressed through the only one dimensionless parameter C. A boxlike potential well leads to similar results with $\lambda=1+(2/\pi)\sqrt{C}$.

Now let us approximate the potential $V_{\rm Sch}(x)$, defined by Eq. (30), by the PT potential (33). First we note that for the SG model the potential $V_{\rm Sch}(x)$ has exactly the form of the PT potential (33) with the parameters $C=C_{\rm SG}=2$ and $\lambda=2$. Therefore, the SG model has only one bound state, the Goldstone mode, while the energy of the second eigenmode coincides with the bottom of the continuum spectrum $E_2=0$ (or $\omega_2=\omega_{\min}$).

For the PR potential (5), we can define $b=d_{\rm eff}$ and V_0 from Eq. (32), so that the parameter C can be determined as

$$C_{\rm PR}=2\frac{(1-r)(1+r^2)}{(1+r)^3}. \tag{34}$$

For $r<r_2=0$ we have $C_{\rm PR}>C_{\rm SG}=2$ and $\lambda>2$. Therefore, the FK model with the PR potential (5) should have the second bound state with the energy

$$E_2\approx-\left(\frac{\lambda-2}{\omega_{\min}d}\right)^2. \tag{35}$$

Thus the FK model with the PR potential (5) always possesses the kink's second internal mode for $r<0$ and its frequency can be found explicitly for small values of r,

$$\omega_2\approx\left\{\omega_{\min}^2-\left(\frac{\lambda-2}{\omega_{\min}}\right)^2\right\}^{1/2}\approx\omega_{\min}-\frac{32r^2}{9\omega_{\min}}. \tag{36}$$

Figure 7 shows the spectrum around a kink for $r\leqslant 0$ and $d=3$ corresponding to rather broad kinks close to the continuum limit. It indicates that the kinks do have at least one localized mode in addition to the Goldstone mode, with vanishing frequency that does not appear on the figure. For $r<0$ but very close to 0, the frequency of the localized mode is well approximated by Eq. (36). For lower values of r, for which other localized modes appear as described below, the approximate expression, which gives the mode that is the closest to the phonon band, is unable to follow the variation of the frequency of one specific mode versus r because it tends to jump from one mode to another. With a further decrease of r, $r<r_3\approx-0.2$, when $C_{\rm PR}>6$ and $\lambda>3$, a third localized mode appears and so on. Figure 7 shows that the analytical predictions are well confirmed by exact numerical calculations.

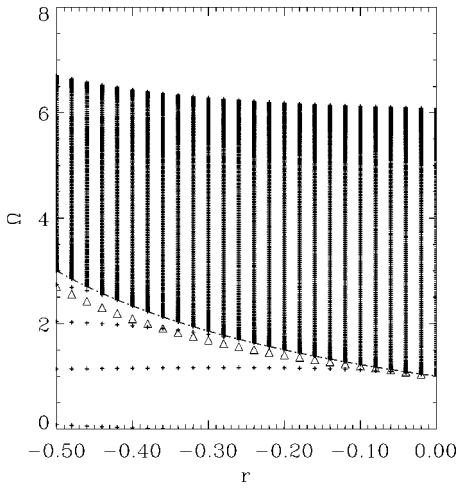

FIG. 7. Spectrum of quasicontinuous kinks ($d=3$) as a function of the shape parameter r. The crosses are the frequencies of the linear modes around the kinks, determined numerically. The PN mode has almost the frequency 0 and is not visible on the figure. The triangles indicate the frequency of the kink's internal mode that is the closest to the lower limit of the phonon band, calculated analytically in the strong-coupling limit.

Now we take into account discreteness effects, assuming, however, that they are small. As is known [7,17,18,23], discreteness leads to narrowing of the kink's width, which approximately can be written in the form

$$d\to d_{\rm discr}\approx d\left[1-\frac{1}{12}\left(\frac{a_s}{d}\right)^2\right]. \tag{37}$$

As a result, the well of the Schrödinger potential (30) will be narrowed, leading to a renormalization of the parameter C,

$$C\to C_{\rm discr}\approx C\left[1-\frac{1}{12}\left(\frac{a_s}{d}\right)^2\right]^2. \tag{38}$$

Therefore, this effect leads to an increase of all eigenvalues of Eq. (29) and therefore to an increase of the eigenfrequencies corresponding to the internal modes. First, the Goldstone mode becomes the PN mode with a nonzero frequency $\omega_1=\omega_{\rm PN}$. Second, the kink's internal mode can exist only for $r\leqslant r_2$, where r_2 is a nonzero negative value. Analogously, the critical values of r at which the higher-order modes show up become shifted to more negative values of r.

Such a shift can be seen by comparing the results of Fig. 7, at $d=3$, and those of Fig. 1(b), at $d=1.5$.

C. Weakly perturbed SG kink

A general condition for the creation of the kink's internal modes can be derived only for the limit of the SG equation perturbed by a small additional term. To show this, we consider the renormalized perturbed SG equation of the form

$$\frac{\partial^2 u}{\partial t^2}-\frac{\partial^2 u}{\partial x^2}+\sin u+\varepsilon g(u)=0, \tag{39}$$

where ε is a small parameter and the function $g(u)$ is a correction to the sinusoidal potential (which can also include derivatives, etc.). First, we look for the kink solution $u_k(x)$ of Eq. (39) by means of the perturbative expansions $u_k(x)=u_k^{(0)}(x)+\varepsilon u_1(x)+\cdots$, where $u_k^{(0)}(x)$ is the kink solution of the SG equation. The correction u_1 can be found in an explicit form

$$u_1(x)=\frac{1}{\cosh x}\int_0^x dx'\cosh^2 x\int_0^{x'}\frac{g(u_k^{(0)})}{\cosh x''}dx''.$$

To analyze the small-amplitude excitations around the kink $u_k(x)$, we linearize Eq. (39) by substituting $u(x,t)=u_k(x)+w(x)e^{i\omega t}$, so that the equation for the function w takes the form

$$\frac{d^2 w}{dx^2}+\frac{2}{\cosh^2 x}w-w+\omega^2 w+\varepsilon\,\delta(x)w=0, \tag{40}$$

where

$$\delta(x)=\sin[u_k^{(0)}(x)]u_1(x)-g'[u_k^{(0)}(x)]. \tag{41}$$

An analysis of the spectral problem (40) can be carried out by means of the singular perturbation theory and allows one to find an additional eigenvalue of the discrete spectrum ω_2, which splits from the edge of the continuum spectrum band under the action of the external perturbation $\sim\varepsilon$ (details of this calculation will be discussed elsewhere [24]). The result is $\omega_2^2=\omega_{\min}^2-\varepsilon^2\kappa^2$, where $\omega_{\min}$ is the lowest frequency of the phonon band (which can be also shifted by the perturbation) and the parameter κ is defined by the expression

$$\kappa=\frac{1}{2}\int_{-\infty}^{+\infty}dx\ \tanh x[\,\delta(x)-\delta(\infty)]\tanh x>0, \tag{42}$$

where $\delta(x)$ can be an operator, and $\delta(\infty)$ is the limiting value of the function (41), which takes into account a shift of the phonon band under the action of the perturbation $\varepsilon g(u)$.

Therefore, a small perturbation applied to the SG equation can give rise to a kink's internal mode provided $\kappa>0$. For the DSG model the application of Eq. (42) gives the result already obtained above; see Eq. (36).

Finally, it is interesting to note that the result (42) is similar to the well-known result of quantum mechanics that a one-dimensional well always has at least one discrete eigenvalue. For the case of the kink's internal mode, an additional eigenvalue appears without a threshold for $\kappa>0$ due to a deformation of the reflectionless potential corresponding to the exact SG kink.

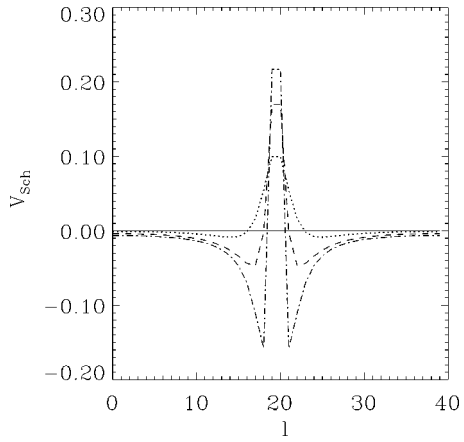

FIG. 8. Potential $V_{\rm Sch}(x)$ of the pseudo-Schrödinger equation for the kink's high-frequency internal modes in the strong-coupling limit ($d=5$) at $r=0.2$ (dotted line), $r=0.4$ (dashed line), and $r=0.6$ (dash-dotted line).

D. Kink's high-frequency internal modes

Because for high-frequency modes the nearest particles oscillate approximately with opposite phases, it is natural to look for a solution of the motion equation (3) in the form (28) with $\delta u_l=(-1)^l\delta v_l$ and then to use the continuum approximation, assuming $\delta v(x)$ to be a slowly varying function. In this way we again obtain the pseudo-Schrödinger equation for the function $\delta v(x)$ analogously to Eq. (29), but with the effective potential of the form

$$V_{\rm Sch}(x)=d^{-2}\{-V''_{\rm sub}[u^{\rm kink}(x)]+V''_{\rm sub}(0)\} \tag{43}$$

and the corresponding eigenvalue (effective ''energy'')

$$E=d^{-2}(\omega_{\max}^2-\omega^2). \tag{44}$$

Note that now the function $V''_{\rm sub}$ enters into the potential (43) with a negative sign, meaning that the bound states with $E<0$ describe the HF localized modes with the frequencies above the upper edge of the phonon spectrum band $\omega>\omega_{\max}$. As is shown in Fig. 8, for the PR potential (5) with $r>0$ the function (43) always has two symmetric potential wells separated by a maximum. For small r the wells are very shallow and the potential may not have a bound state. According to the well-known result of quantum mechanics, this corresponds to the total area calculated for the potential $V_{\rm Sch}(x)$ to be positive.

As r increases, the minima become deeper and a bound state emerges from the top of the phonon band, as shown in Fig. 9(a). As it is the lowest state of the pseudo-Schrödinger equation with an even potential, it must have an even symmetry $\delta v(x)=\delta v(-x)$. This is confirmed by numerical calculations of its eigenvector, as shown in Fig. 9(b). As r increases further, the wells become deeper and additional bound state appears as an odd solution with a slightly higher eigenvalue; see Fig. 9(c). The mode with the highest frequency $\omega_M>\omega_{\max}$ is the kink's internal mode, which de-

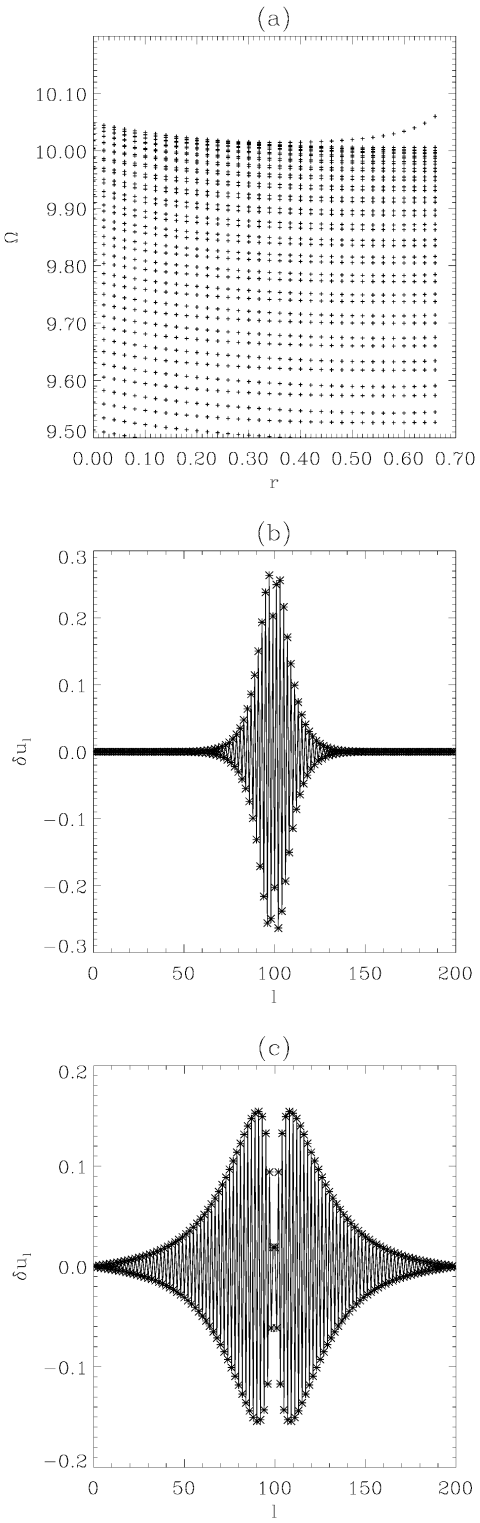

FIG. 9. Kink's high-frequency internal modes in the strong-coupling limit. (a) Spectrum of the small-amplitude excitations around the kink vs the potential parameter r for $d=5$. Only the region corresponding to the top of the phonon band is shown. (b) Eigenvector of the mode with the highest frequency for $r=0.6$. It is a localized mode with even symmetry. (c) Eigenvector of the mode with a frequency immediately below. It is also a localized mode, but as its frequency is very close to the top of the phonon band as shown in Fig. 9(a), it is only weakly localized. This mode has an odd symmetry.

scribes in-phase oscillations of the kink wings, while other more complicated modes correspond to lower frequencies.

V. KINK'S NONLINEARITY-INDUCED INTERNAL MODES

The analysis presented above is based on the linear approximation when the amplitude of the kink's internal oscillations is assumed to be small. For larger amplitudes the oscillations become anharmonic and we should take into account nonlinear effects.

First we recall that for the FK chain without a kink LF or HF intrinsic nonlinear localized modes can exist (see, e.g., Ref. [2]); the LF mode is an analog of a breather of the SG model, while the HF mode appears due to the discrete nature of the FK model. In addition, for the FK chain with an impurity, nonlinear impurity modes can also exist [11]. In both these cases the frequency of LF mode decreases, while the frequency of the HF mode increases, with a growth of the oscillation amplitude. It is natural to expect similar effects for the kink's internal modes, i.e., a nonlinearity-induced shift of the mode frequencies. Such a shift of the frequency due to a self-localization effect may have the following important consequences. If in the linear approximation the kink's internal mode is a virtual mode, i.e., its frequency is in the phonon band but close enough to one of the band edges, this mode can be transformed into a local mode with the frequency lying outside the phonon band for larger oscillation amplitudes. Thus the number of internal kink modes will increase with increasing amplitude of the kink's oscillations.

In general, the nonlinearity of a given shape mode is expected to have two main consequences: the excitation of higher harmonics and a frequency shift as a function of the amplitude. The first effect, i.e., the excitation of higher-order harmonics, may have a dramatic effect if they fall within the phonon band because they provide channels for radiative decay. This is the case for the PN mode when its frequency is above the value $\omega_{\min}/2$. Let us illustrate this by an example for $r=0.1$ and $d=1$ for which the PN mode has the frequency $\omega_{\mathrm{PN}}=0.5386$ while the phonon band $\omega_{\min}\leqslant\omega\leqslant\sqrt{\omega_{\min}^2+4d^2}$, with $\omega_{\min}=(1-r)/(1+r)$, is situated in the range $0.8182\leqslant\omega\leqslant 2.1609$. We simulate the dynamics of a kink with an excited PN mode by solving the equations of motion (3) with the initial condition

$$u_l(t=0)=u_l^{\mathrm{eq}}+Av_l^{\mathrm{PN}}, \tag{45}$$

where v_l^{PN} are the displacements of the particles corresponding to a normalized linear PN mode and $\Sigma(v_l^{\mathrm{PN}})^2=1$, obtained numerically by diagonalizing the dynamical matrix of the small-amplitude oscillations as described in Sec. III. The parameter A determines the amplitude of the excitation of the mode. For small A (such as $A=0.001$) the linearized description is valid and the numerical simulations confirm the stability of the mode. We follow the amplitude of the oscillation of the kink in the PN potential by recording the motion of the particles that are on both sides of the center. As shown in Fig. 10(a), the amplitude of the oscillations of these particles around their equilibrium positions stays constant with time. The measurement of the frequency of the oscillation derived from a Fourier transform of the time evolution of the posi-

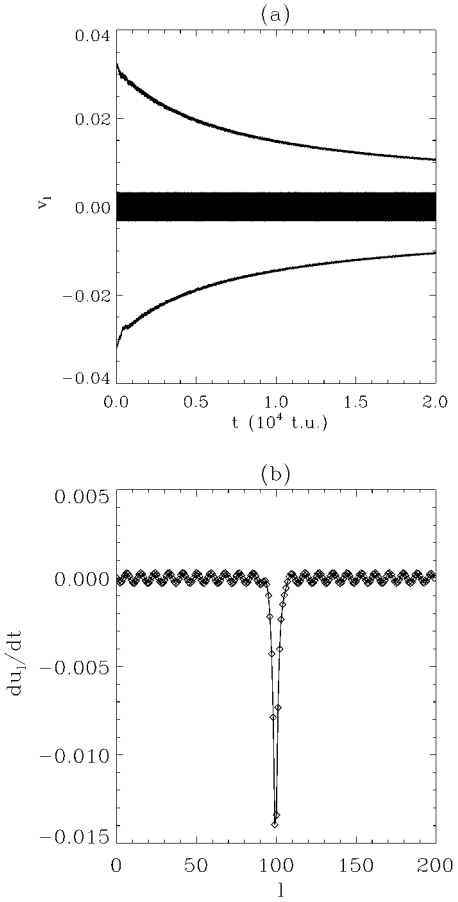

FIG. 10. Numerical studies of the time evolution of a kink with an excited PN mode for $r=0.1$ and $d=1.0$. The initial condition is given by Eq. (45). (a) Time evolution of the displacement of a site adjacent to the kink center. Only the difference between the equilibrium position and the instantaneous position of the particle is shown. This figure combines the result of two simulations with two initial conditions. (i) $A=0.001$. The time evolution of the particle displacements appears on the figure as a thick black line around $v_l=0$ because the period of the oscillation is very small at the scale of the figure ($0\leqslant t\leqslant 20\,000$) and the sinusoidal oscillation of the displacement cannot be seen. The thickness of the line shows the amplitude of the oscillation. To make this amplitude visible on the plot, it is magnified by a factor of 10. One can notice that the amplitude of the oscillation stays constant as time evolves. (ii) $A=0.1$. For this larger excitation the amplitude of the PN mode decays with time. The figure shows only the extrema of the particle displacements. The positive and negative extrema of the oscillation generate the two exponentially decaying curves on the plot. (b) Snapshot of the velocities of the particles at $t=10\,000$ for the initial condition with $A=0.1$. The emission of small-amplitude waves away from the kink center appears clearly on the figure. A damping term (with the coefficient $\gamma=0.1$) is added to the equations for the last ten sites at both ends of the chain to avoid a reflection of the waves at the fixed ends.

tion of one of these particles gives $\omega=0.538\,51\pm0.000\,31$, in good agreement with the frequency $\omega_{\mathrm{PN}}=0.538\,58$ obtained by a numerical investigation of the spectrum of the small-amplitude oscillations around the kink. Although the Fourier spectrum detects a tiny contribution of the second harmonic, it is so small that it does not play any measurable role in the system dynamics. On the contrary, for $A=0.1$ the simulation shows a significant decay of the amplitude of the PN mode, as shown in Fig. 10(a). The Fourier spectrum gives a frequency of $\omega=0.538\,20\pm0.000\,31$. This indicates a slight decay of the frequency of the PN mode when its amplitude increases. Moreover, the Fourier spectrum indicates a larger contribution of the second harmonic, which is within the phonon band and therefore induces the emission of small-amplitude propagating waves that carry energy away from the kink [see Fig. 10(b)]. This emission explains the decay of the amplitude of the PN mode.

As discussed above, we also expect that *nonlinearity can localize a mode* that would not be localized in the linear lattice. We have checked numerically that this effect is indeed possible. An example is presented in Figs. 11(a)–11(c). We consider a kink in the discrete SG equation, i.e., at $r=0$ and $d=2$. Figure 11(a) shows the shape of the first mode above the PN mode, i.e., the mode that corresponds to the bottom of the phonon band. An initial condition for the simulation is generated by adding to the equilibrium displacements corresponding to the eigenvector v_l^{PH} of this mode, with an amplitude factor $A=0.5$,

$$u_l(t=0)=u_l^{\mathrm{eq}}+Av_l^{\mathrm{PH}}. \tag{46}$$

Figure 11(b) shows that after an initial decay because the initial condition is not an exact solution of the system, the amplitude of the kink's oscillations, observed through the displacements of the particle adjacent to the center, settles to a value that oscillates but has a constant average. A snapshot of the velocities of the particles [see Fig. 11(c)] shows that the displacements around the kink have now the *characteristic shape of a local mode*. They decay exponentially away from the center. The measurement of the frequency of the large-amplitude shape mode created by this process gives $\omega=0.995\,98\pm0.000\,78$, i.e., a frequency that is below the bottom of the phonon band, $\omega_{\mathrm{min}}=1.0$ for the discrete SG chain. The slow oscillation of the amplitude of the shape mode that appears in Fig. 11(a) is a beating between the mode localized by nonlinearity and a mode at the bottom of the phonon band that persists in the system because the simulation started from an initial condition that does not correspond exactly to the excited kink. The extra contribution near the bottom of the phonon band has a vanishing group velocity and stays around the kink's center, causing the beating. Therefore, increasing the amplitude of the lowest mode of the phonon band has turned it to a local mode due solely to the nonlinearity-induced frequency shift.

A similar localization due to nonlinearity is possible for a high-frequency localized mode, although this effect is more difficult to observe numerically. Figures 12(a) and 12(b) show an example for $d=2$ and $r=0.23$. This value of r was chosen because, although the corresponding kink does not have a linearized, localized, HF mode, a small increase in r (up to $r=0.25$) is sufficient to create such a mode. Therefore, although we start from an approximate initial condition, we can expect to create a localized mode for $r=0.23$ if we increase the amplitude of excitation of the mode at the top of the phonon band enough to make it nonlinear. The results of Figs. 12(a) and 12(b) show that it is indeed possible. The mode shown in Fig. 12(a) was excited with an amplitude factor $A=3$. A plot of the velocities of the particles at

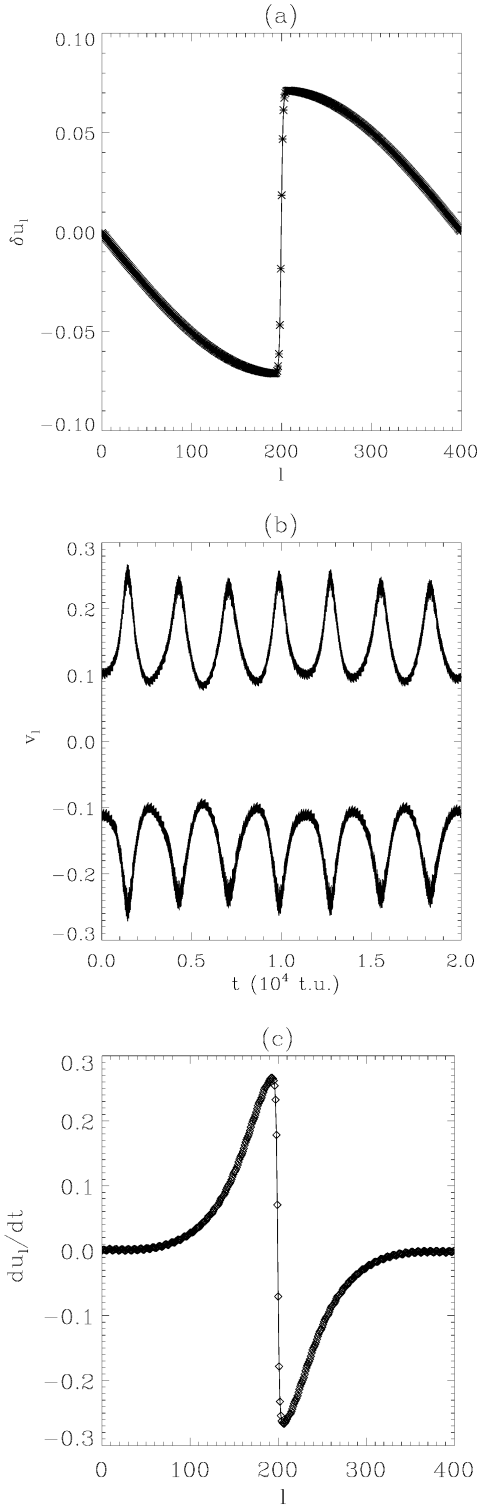

FIG. 11. Nonlinearity-induced localization of a low-frequency mode around a kink for $r=0$ and $d=2$. (a) Eigenvector of the linearized mode that is situated above the PN mode. This mode corresponds to the bottom of the phonon band. Its frequency is equal to $\omega=1.000\,12$ (due to the finite size of the system the true bottom of the phonon band at $\omega=1.0$ is not observed). (b) Time evolution of the amplitude of the oscillations of the particles adjacent to the kink center in a simulation with an initial condition including the equilibrium kink and the mode shown in (a) with an amplitude $A=2.5$. Only the extrema of the displacements are shown. (c) Snapshot of the velocities of the particles at $t=15\,000$ time units.

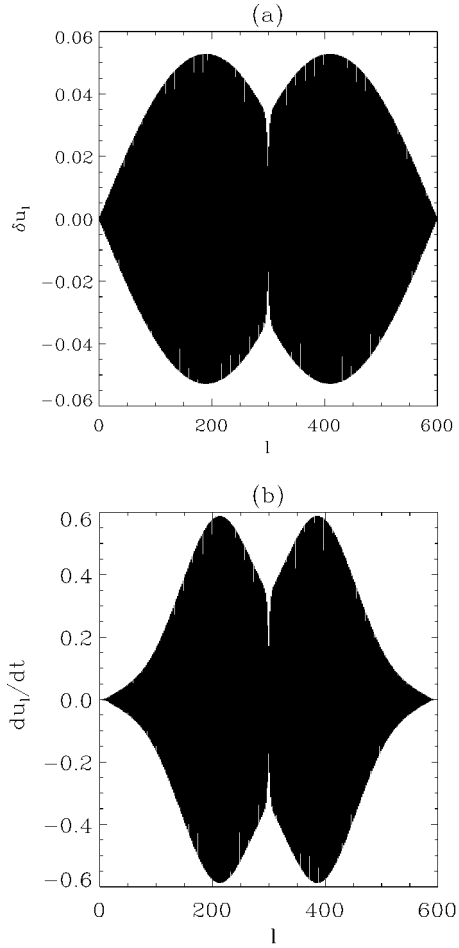

FIG. 12. Nonlinearity-induced localization of a high-frequency mode around a kink for $r=0.23$ and $d=2$. (a) Eigenvector of the linearized mode around the kink that corresponds to the top of the phonon band. Its frequency is equal to $\omega=4.048\,657\,1$. (b) Snapshot of the velocities of the particles at $t=25\,000$ time units.

$t=15\,000$ time units [see Fig. 12(b)] shows that the mode has acquired a shape with exponentially decaying tails, characteristic of a local mode. The variation of frequency is small, $\omega=4.048\,998\pm0.000\,959$, i.e., it is above the initial value of 4.048 657 1 corresponding to the top of the phonon band.

VI. CONCLUSIONS

We have investigated the effect of discreteness on the existence and properties of a kink's internal modes in the generalized FK models. We have shown that there exists a simple qualitative analogy between the kink's internal modes and impurity modes and we have employed this analogy to discuss the physics and origin of these localized modes of kinks in discrete lattices. We have used two different methods to describe the kink's internal modes analytically in the limiting cases of weak (strongly discrete) and strong (continuum approximation) interactions between the particles in the lattice. We have revealed and described two important physical effects associated with the kink's internal modes: high-frequency localized kink oscillations above the phonon

band of a discrete lattice and nonlinear kink internal modes that can appear due to a nonlinearity-induced frequency shift from the upper and lower edges of the phonon spectrum band. We believe the main features of the kink's internal modes analyzed here for some particular examples of the generalized FK model will be found also in other discrete physical systems.

ACKNOWLEDGMENTS

O.B. is indebted to A. S. Kovalev for useful discussions. Yu.K. is a member of the Australian Photonics Cooperative Research Center. He also acknowledges useful discussions with Dmitry Pelinoivsky and partial support of the Australian Academy of Science through the Bede Morris Fellowship Program.

[1] Ya. Frenkel and T. Kontorova, Fiz. Zh. (Moscow) **1**, 137 (1938); Phys. Z. Sowjetunion **13**, 1 (1939).
[2] O. M. Braun and Yu. S. Kivshar, Phys. Rep. (to be published).
[3] A. Seeger and A. Kochendörfer, Z. Phys. **130**, 321 (1951); J. K. Perring and T. H. R. Skyrme, Nucl. Phys. **31**, 550 (1962); M. J. Ablowitz, D. J. Kaup, A. C. Newell, and H. Segur, Phys. Rev. Lett. **31**, 125 (1973); L. A. Takhtadzhyan and L. D. Faddeev, Teor. Mat. Fiz. **21**, 160 (1974).
[4] M. Peyrard and M. Remoissenet, Phys. Rev. B **26**, 2886 (1982).
[5] M. Peyrard and D. K. Campbell, Physica D **9**, 33 (1983); D. K. Campbell, J. F. Schonfeld, and C. A. Wingate, *ibid.* **9**, 1 (1983); D. K. Campbell, M. Peyrard, and P. Sodano, *ibid.* **19**, 165 (1986).
[6] Yu. S. Kivshar, Fei Zhang, and L. Vázquez, Phys. Rev. Lett. **67**, 1177 (1991); Phys. Rev. A **46**, 5214 (1992).
[7] Y. Ishimori and T. Munakata, J. Phys. Soc. Jpn. **51**, 3367 (1982); M. Peyrard and M. D. Kruskal, Physica D **14**, 88 (1984).
[8] C. A. Condat, R. A. Guyer, and M. D. Miller, Phys. Rev. B **27**, 474 (1983).
[9] I. M. Lifshitz, J. Phys. (Moscow) **7**, 215 (1943); **7**, 249 (1943); **8**, 89 (1944).
[10] A. A. Maradudin, *Theoretical and Experimental Aspects of the Effects of Point Defects and Disorder on the Vibrations of Crystals* (Academic, New York, 1966).
[11] O. M. Braun and Yu. S. Kivshar, Phys. Rev. B **43**, 1060 (1991).
[12] R. Peierls, Proc. Phys. Soc. London **52**, 34 (1940).
[13] F. R. N. Nabarro, Proc. Phys. Soc. London **59**, 256 (1947).
[14] R. Giachetti, P. Sodano, E. Sorace, and V. Tognetti, Phys. Rev. B **30**, 4014 (1984).
[15] P. Sodano, M. El-Batanouny, and C. R. Willis, Phys. Rev. B **34**, 4936 (1986).
[16] C. R. Willis, M. El-Batanouny, S. Burdick, and R. Boesch, Phys. Rev. B **35**, 3496 (1987).
[17] J. F. Currie, S. E. Trullinger, A. R. Bishop, and J. A. Krumhansl, Phys. Rev. B **15**, 5567 (1977).
[18] S. De Lillo, Nuovo Cimento B **100**, 105 (1987).
[19] R. Boesch, C. R. Willis, and M. El-Batanouny, Phys. Rev. B **40**, 2284 (1989).
[20] R. Boesch and C. R. Willis, Phys. Rev. B **39**, 361 (1989).
[21] H. Segur, J. Math. Phys. (N.Y.) **24**, 1439 (1983).
[22] G. Pöschl and E. Teller, Z. Phys. **83**, 143 (1933); S. Flügge, *Practical Quantum Mechanics I* (Springer-Verlag, Berlin, 1971), Sec. 39.
[23] C. R. Willis, M. El-Batanouny, and P. Stancioff, Phys. Rev. B **33**, 1904 (1986).
[24] Yu. S. Kivshar, D. E. Pelinovsky, and M. Peyrard (unpublished).